Article

Heavy Metals in Pyrolysis of Contaminated Wastes: Phase Distribution and Leaching Behaviour

Erlend Sørmo [1,2,*], Gabrielle Dublet-Adli [1], Gladys Menlah [2], Gudny Øyre Flatabø [3,4], Valentina Zivanovic [2], Per Carlsson [3], Åsgeir Almås [2] and Gerard Cornelissen [1,2]

1 Geotechnics and Environment, Norwegian Geotechnical Institute (NGI), 0484 Oslo, Norway; gerard.cornelissen@ngi.no (G.C.)
2 Faculty of Environmental Sciences and Natural Resource Management, Norwegian University of Life Sciences (NMBU), 1433 Ås, Norway; valentina.zivanovic@nmbu.no (V.Z.)
3 Scanship Innovation Lab VOW ASA, 1384 Asker, Norway; per.carlsson@vowasa.com (P.C.)
4 Faculty of Technology, Natural Sciences and Maritime Sciences, University of South-Eastern Norway (USN), 3918 Porsgrunn, Norway
* Correspondence: erlend.sormo@ngi.no

Abstract: Pyrolysis is a recognized alternative for the sustainable management of contaminated organic waste, as it yields energy-rich gas, oil, and a carbon-rich biochar product. Low-volatility compounds, however, such as heavy metals (HMs; As, Cd, Cu, Cr, Ni, Pb, and Zn) typically accumulate in biochars, limiting their application potential, especially for soil improvement. The distribution of HMs in pyrolysis products is influenced by treatment temperature and the properties of both the HMs and the feedstock. There is a significant knowledge gap in our understanding of the mass balances of HMs in full-scale industrial pyrolysis systems. Therefore, the fate of HMs during full-scale relevant pyrolysis (500–800 °C) of seven contaminated feedstocks and a clean wood feedstock were investigated for the first time. Most of the HMs accumulated in the biochar (fixation rates (*FR*) >70%), but As, Cd, Pb, and Zn partly partitioned into the flue gas at temperatures ≥ 600 °C, as demonstrated by FRs of <30% for some of the feedstocks. Emission factors (EFs, mg per tonne biochar produced) for particle-bound HMs (<0.45 μm) were 0.04–7.7 for As, 0.002–0.41 for Cd, 0.01–208 for Pb, and 0.09–342 for Zn. Only minor fractions of the HMs were found in the condensate (0–11.5%). To investigate the mobility of HMs accumulated in the biochars, a novel leaching test for sustained pH drop (at pH 4, 5.5 and 7) was developed. It was revealed that increasing pyrolysis temperature led to stronger incorporation of HMs in the sludge-based biochar matrix: after pyrolysis at 800 °C, at pH 4, <1% of total Cr, Cu, Ni, and Pb and < 10% of total As and Zn contents in the biochars were leached. Most interestingly, the high HM mobility observed in wood-based biochars compared to sewage-sludge-based biochars indicates the need to develop specific environmental-management thresholds for soil application of sewage-sludge biochars. Accordingly, more research is needed to better understand what governs the mobility of HMs in sewage-sludge biochars to provide a sound basis for future policy-making.

Keywords: pyrolysis; organic waste; heavy metals; biochar; emission factors; leaching

1. Introduction

Pyrolysis, which entails heating in the absence of oxygen, has gained attention from researchers and legislators over the last two decades as a potential sustainable strategy for managing organic waste [1–4]. The main reasons are that pyrolysis of organic waste produces energy-rich pyrolysis gas, pyrolysis condensates, and biochar—a porous, carbon-rich product with a versatile set of characteristics. These characteristics include high water retention [5,6] nutrient retention [7], pH-buffering capacity [8], and a carbon capture and storage effect [9], all of which have caused biochar to be identified as suitable for use in agricultural soil improvement. More recently, biochars have been recognized as sorbents for

environmental contaminants [10–13], fillers in concrete [14], soil-stabilizing agents [15] and substitutes for anthracite coal in the metallurgical industry [16]. Pyrolysis is furthermore being explored as a strategy for managing contaminated wastes [17–21].

A potential drawback of using pyrolysis for waste handling to produce biochar is that non-volatile species such as various metal(oid)s like As, Cu, Pb, and Zn are enriched in the biochar product [19–23]. The fixation of a metal(oid) in biochar depends on its initial concentration and speciation in the feedstock, its physicochemical properties, and the composition and extent of mass reduction of the feedstock matrix (biochar yield) [23]. The composition of the feedstock matrix significantly affects pyrolysis outcomes [24,25]. Biochar yield decreased exponentially with increasing pyrolysis temperatures for a number of different feedstocks, with the exception of sewage-sludge feedstocks, in which the decrease was less pronounced due to a large fraction of inorganic elements [26]. Melting and boiling points of metal(oid)s influence their degree of fixation and volatilization upon pyrolysis, but the feedstock matrix greatly affects the process through redox reactions and formation of composite species [22,27,28]. For example, Cd and Pb are thought to be volatilized through reactions with the carbon matrix of the feedstock [22], but the presence of Cl or S in the feedstock affects this process by forming more volatile chloride-species or less volatile sulphide species [27]. One of the most volatile metal(oid)s, is As, with volatilization starting at <500 °C in the presence of organic carbon [22]. However, the presence of Ca or Fe can counteract volatilization by formation of e.g., $CaAsO_2$ [29] or FeAs [30]. Due to complex interactions between metal(oid) properties and the feedstock matrix, predicting their distribution in pyrolysis products is challenging. For pyrolysis to be adopted as a realistic treatment option for contaminated organic wastes, more knowledge about how metal(oid)s distribute in biochar, pyrolysis condensate, and flue gas from such feedstocks is needed. There is a special need to quantify potential metal(oid)s in flue-gas emissions, as such information is deficient in the current literature.

High metal(oid) concentrations in biochar can limit its applications. This is especially true in cases with high concentrations of the heavy metals (HMs), As, Cd, Cr, Cu, Hg, Ni, Pb, and Zn. Threshold levels for HMs in biochars intended for agricultural-soil application have been suggested by the European Biochar Certificate [31] and by a technical panel for the European Union (EU) Fertilising Products Regulation [32]. These threshold levels are based on total concentrations of HMs, which are useful indicators of overall contamination, although they are not as relevant for assessing environmental risk [33,34]. Different methods have been developed to predict the soluble fractions of metals for risk-assessment purposes, such as water-extractable compounds [21,35] sequential extractions [19,36], the Toxicity Characteristic Leaching Procedure (TCLP) [37,38], and leaching tests with altered pH [39,40]. These studies generally agree that most HMs do not readily leach due to the alkaline pH of the biochars. Pyrolysis temperature seems to correlate negatively with HM mobility, as increased temperatures increase inclusion of HMs in insoluble fractions such as Fe-Mn nodules, sulphides, and silicate minerals [38,41]. However, the leaching methods typically applied are operationally defined and were not developed to test biochars specifically. Hence, they might fail to accommodate properties unique to biochars, such as complex buffering capacities [42]; this may, e.g., result in the biochar buffering added acid so that the addition produces no or little change in pH rather than releasing an acid-soluble fraction, as experienced by Kistler et al. [39]. Through application, e.g., in acidic soils or wastewater treatment, HM-rich biochars might experience a sustained change in pH. An exploration of the pH-dependent leachability of HMs could therefore add important insights to the environmental risk of waste biochar application. Such an exploration would require a new approach to the leaching test, where acidification is done in accordance with the buffer capacity of the biochar material investigated. This would require sufficient amounts of acid to break the buffer capacity and hence achieve a sustained reduction in pH for the duration of the leaching test.

This study utilized a full-scale relevant unit (2–5 kg biochar hr^{-1}) to pyrolyze eight different organic waste feedstocks (wood and sludge-based) at temperatures ranging from

500 to 800 °C. The main aim was to document the distribution of heavy metals across pyrolysis products and study the pH-dependent mobility of heavy metals accumulated in the biochars produced. The following hypotheses were tested: (1) a high pyrolysis temperature volatilizes Cd, Cu, Pb, and Zn into the flue gas, but the effect is matrix-dependent, and (2) a high pyrolysis temperature is beneficial for producing insoluble metal species in the biochars that will not leach upon a sustained drop in pH. To the best of our knowledge, our study is the first to report a mass balance including emission factors for HMs as a function of both diverse waste feedstocks and different pyrolysis temperatures. Further novelty is added by demonstrating and applying a method for leaching HMs from biochars following a sustained drop in pH.

2. Materials and Methods

The waste fractions investigated and their respective pyrolysis treatments in the present work were the same as those described in two related studies by Sørmo et al. [43,44]. These two studies investigated the fate of per and polyfluorinated alkylsubstances (PFAS) and the fate of polychlorinated biphenyls (PCBs), dibenzodioxins and furans (PCDD/Fs), and polycyclic aromatic hydrocarbons (PAHs), respectively. It was found that >96% of target PFAS and >99% of target PCDD/Fs and PCBs were removed from the waste feedstocks in the transformation to biochar at pyrolysis temperatures $\geq$ 500 °C. In the present work, however, the focus was the fate of inorganic elements, but the sample collection and emissions measurements were done in parallel with the already published sampling of organic contaminants. Thus, details of the process can be found in Sørmo, Castro et al. [43], while a summary has been included in the following sections.

2.1. Chemicals and Materials

Double-distilled HNO_3, HCl, and HF (trace-metal-analysis quality, Merck, Darmstadt, Germany) were used for pH adjustment and for decomposition of samples. Polypropylene tubes (PP, 50 mL, Sarstedt, Germany) were used for dilution after decomposition and for leaching tests. Whatman® cellulose filters (0.45 μm) purchased from VWR (Trondheim, Norway) were used for leachate filtration. Single-element standard solutions of each element investigated (1000 mg L^{-1}, Inorganic Ventures, Christiansburg, VA, USA) were used to prepare calibration solutions for elemental analysis. Deionized water 18 MΩ cm^{-1} produced in the laboratory (Barnstead) was used for leaching tests, in addition to washing, dilution, and preparation of standard solutions.

2.2. Organic Waste Feedstocks

The feedstocks tested included seven contaminated organic wastes (Table 1): two digested sewage sludges (DSS-1 and DSS-2), limed sewage sludge (LSS), de-watered raw sewage sludge (DWSS), food-waste reject (FWR), waste timber (WT), and garden waste (GW). Wood-chip pellets (clean wood chips, CWC) were used as an uncontaminated reference material. Samples of each feedstock were collected in bulk (2 m³) before drying (to 5–10% moisture content) in a batch paddle dryer (1.5 × 5 m) built by Scanship AS (now part of VOW ASA, Lysaker, Norway). In this setup, the feedstocks were dried at 102–110 °C through heating supplied by a heat exchanger, which was channelled into a heating jacket fitted around the dryer. Dry feedstocks were then pelletized (length 40 mm, radius 8 mm) before pyrolysis.

Table 1. Description of waste-material feedstocks used in the present study and conditions for their pyrolysis treatment.

Category	Feedstock	Abbrev.	Description	Treatment Temp. (°C)	Retention Time (min)	Biochar Samples	Pyrolysis Oil Samples	Emission Samples	Leaching Data
Wood-based	Wood chips	CWC	Pellets produced from wood chips from forestry/logging.	530, 600, 700 and 750	20	Yes, for all treatments	Yes, for 600 °C treatment	Yes, for all treatments	Yes, for all treatments
	Waste timber	WT	Discarded wood products and objects from private households, businesses, and construction/demolition (no chemically impregnated wood)	500, 600, 700 and 800	20	Yes, for all treatments	Yes, for 600, 700 and 800 °C treatments	Yes, for all treatments	Yes, for all treatments
	Garden waste	GW	Gardening waste from private households and businesses. Fraction includes twigs, leaves, roots, and some sand/gravel.	500, 600 and 800	20	Yes, for all treatments	Yes, for all treatments	Yes, for 500 and 800 °C treatments	No
Food waste	Reject from food waste biogas production	FWR	Fraction of food-waste rejected from biogas production. Consists of material that does not pass an initial sieving process to reject plastics and other too-large or non-digestible items.	600 and 800	20	Yes, for all treatments	Yes, for 800 °C treatment	Yes, for all treatments	No
Sewage sludge and food waste	Digested sewage sludge	DSS-1	Sewage sludge and food waste that has gone through thermal hydrolysis (155 °C, 20 min) before anaerobic digestion for biogas production	500, 600, 700 and 770	20	Yes, for all treatments	Yes, for 500, 600 and 700 °C treatments	Yes, for 500, 600 and 700 °C treatments	Yes, for all treatments
Sewage sludge	Digested sewage sludge	DSS-2	Sewage sludge that has gone through anaerobic digestion for biogas production	500, 600, 700 and 800	20	Yes, for all treatments	Yes, for all treatments	Yes, for all treatments	Yes, for all treatments
	Limed sewage sludge	LSS	Sewage sludge that has gone through anaerobic digestion for biogas production, with added lime (39% d.w.) for stabilization/hygenization	600 and 760	20	Yes, for all treatments	Yes, for all treatments	Yes, for all treatments	No
	Dewatered sewage sludge	DWSS	Raw sewage sludge, thermally hydrolyzed (165 °C, 40 min) and then dewatered hot (90 °C) using a centrifuge.	600, 700, 800 and 830	40	Yes, for all treatments	No	No	No

The feedstocks were selected to represent organic waste fractions that are produced in significant quantities (>50,000 tonnes yr^{-1}) [45] and to represent variation in feedstock composition sufficient to produce biochars with distinct properties [24–26].

2.3. Pyrolysis Technology and Operational Conditions

Feedstocks were pyrolyzed using Biogreen® technology made by ETIA Ecotechnologies (now part of VOW ASA, Lysaker, Norway): a medium-scale unit (2–10 kg biochar per hr) with a water-cooled condensation unit (10 °C) for removal of pyrolysis condensate and subsequent pyrolysis gas combustion (700–940 °C) in a propane-supported torch combustor. The Spirajoule©, an electrically heated screw, is the key component of the pyrolysis reactor. The electrical current that runs across and the rotational frequency of the screw regulate pyrolysis temperature and retention time, respectively. The system was flushed with N_2 before start as a means of purging O_2. The reactor operated under negative pressure to allow for a quick separation of the pyrolysis gas from the solid phase. A schematic of the unit is shown in Figure S1.

Feeding rate was adjusted between 5 and 10 kg hr^{-1} to accommodate the physical differences in the various feedstock pellets. Retention time in the pyrolysis reactor was 20 min for all feedstocks and treatments except the DWSS, which was run at 40 min due to technical challenges. Pyrolysis temperature was considered the main treatment variable and was varied between 500 and 800 °C. The lower temperature threshold, 500 °C, was selected in order to ensure efficient decomposition of organic contaminants in the waste feedstocks [44,46–48]. The upper threshold, 800 °C, was the maximum temperature achievable with the Biogreen® technology at the time of operation. It should be noted that the high temperature range selected could lead to elevated emissions of SO_2 and HCl during pyrolysis of sewage sludges [49], so there could be a need for flue-gas cleaning, depending on the scale of the operation. Degradation of organic contaminants might also lead to emissions of degradation products, which is another reason why flue-gas cleaning could be necessary [43,44]. Target temperatures were set at 500, 600, 700, and 800 °C, but operational challenges such as clogging of pipes and burner instability resulted in some deviation from the target temperatures (e.g., for CWC, DSS-1, LSS, and DWSS in Table 1). Due to logistical challenges, including complications during operation and budgetary and time restrictions, not all feedstocks were treated at the full set of target temperatures (see Table 1 for details).

Sampling was conducted only during the period defined as having stable conditions, which lasted about two hours for each treatment. Biochar yield (Y_{BC}) was calculated as the biochar production rate (R_{BC}) divided by the feeding rate (R_F) during stable conditions, as follows:

$$Y_{BC}(\%) = \frac{R_{BC}\left(\text{kg hr}^{-1}\right)}{R_F\left(\text{kg hr}^{-1}\right)} \times 100 \tag{1}$$

2.4. Solids Sampling

Feedstock subsamples for chemical analyses were collected during pelletisation of the bulk sample by random-grab sampling (1 kg, 10–20 scoops). Biochar subsamples were taken by random-grab sampling (1 kg, 10–20 scoops) from the total amount of biochar produced under stable conditions. Samples were air-dried in the laboratory (<1% moisture) before being crushed and homogenized (D < 1 mm, sieved) with a ball mill (Retsch ISO 9001, 50 rpm, 10 min). The ball mill was cleaned between samples; it was first cleaned with soap, then rinsed with MeOH:MilliQ (50%) and dried (105 °C, 30 min).

Pyrolysis condensate was collected under stable conditions. Phase separated condensates were decanted, and the separate fractions were weighed before subsamples (500 mL) were reconstructed. Pyrolysis condensate from sewage-sludge samples, however, did not spontaneously phase-separate, so subsamples were taken after vigorous shaking of the bulk sample.

2.5. Flue-Gas Sampling

Exhaust gas for aerosol measurements was collected from inside the chimney, within the inner 2/3 of the chimney diameter at about 20 cm below the outlet. The chimney is the only exit point for gases and aerosols in the Biogreen unit. The sampling period for each pyrolysis temperature was approximately 2 h. Flue-gas samples could not be collected for all feedstocks and treatment temperatures due to technical challenges that resulted in insufficient sampling time (Table 1).

Emitted aerosols were collected for metal analysis on a cellulose filter (0.45 μm) with a low-volume air sampler (Comde-Derenda, Stahnsdorf, Germany) run at 2.4 m^3 h^{-1}. One cumulative sample (30 min) was collected for each temperature treatment. This unit draws flue gas from the chimney across a filter cartridge using a pump with a flow meter. The filter cartridge was rinsed with MeOH, then MiliQ, between samplings.

Concentrations of carbon-based gases (carbon monoxide (CO), carbon dioxide (CO2), methane (CH4), and non-methane volatile organic carbon (NMVOC = ethane (C2H6) + propane (C3H8) + ethylene (C2H4) + hexane (C6H14) + formaldehyde (CHOH))) in the flue gas were measured (every 3 min) throughout the test using a Fourier Transform Infrared Spectrometer (FTIR, Gasmet, Vantaa, Finland). Particle concentrations (PM$_{10}$) were logged (every 10–20 min) with a pdr-1500 instrument (Thermo Scientific, Waltham, MA, USA). The concentrations of carbon-based gases and aerosols were used as a basis on which to estimate the flue-gas volume as per the carbon-balance approach (see [43,49] for more details).

2.6. Chemical and Structural Characterization

The main element (Ca, Fe, K, Mg, Na, P, S and Si) and trace element (As, Ba, Cd, Co, Cr, Cu, Mo, Ni, Pb, Sr, V and Zn) contents in feedstocks and biochars were determined by digesting triplicate samples in parallel with HNO$_3$ (conc.) and a HNO$_3$ and HF (5:1) at 260 °C in an Ultraclave microwave digestion system (Milestone), with subsequent dilution up to 50 mL and analysis with a Triple QQQ 8800 ICP-MS (Agilent Technologies) with a reaction-collision cell (As, Ba, Cd, Co, Cr, Cu, Mo, Ni, Pb, S, Sr, and V) and a 5100 SVDV ICP-OES (Agilent Technologies) for determination of Ca, Fe, K, Mg, Na, P, Si, and Zn. The cellulose filters were digested only by HNO$_3$ due to limited sample material. The NJV 94-5 (wood-fuel reference material), and NCS ZC 73,007 (soil-certified reference material) were used for control recovery of each element of interest after decomposition and analytical measurements and were all between 5–10%. Limits of detection (LODs) and limits of quantification (LOQs) for all elements analysed are reported in Table S1. All samples were corrected for analytical blanks. Metals in the pyrolysis condensate samples were determined with ICP-OES by the Norwegian Oil Laboratory AS (Rørvik, Norway). Samples were injected directly into the plasma without digestion or sample preparation. Phases were analysed separately for phase-separated samples. The analysis was calibrated for concentrations up to 1500 ppm with a LOQ of 1 ppm.

Feedstock and biochar samples were analysed in triplicate for total carbon using the dry combustion method with IR detection, as described by Nelson & Sommers [50], and total nitrogen by the Dumas method with thermal conductivity, as described by Bremmer & Mulvaney [51], both on a Leco CHN628 instrument. Total carbon content in the pyrolysis condensate samples was determined through combustion with subsequent infrared detection of CO$_2$ species in accordance with method ASTM D5291.

Ash content was determined at 550 °C according to method DIN 51,719 using a Thermogravimetric Analysis setup with an O$_2$ atmosphere and 5 K min^{-1} temperature gradient. pH was measured at a liquid-to-solid ratio of 5 in MilliQ water using a PHM210 (Radiometer, MeterLab®, Terni, Italy). Specific surface area (SSA) and pore volume (PV) were determined on a Quantachrome Autosorb I by both CO$_2$ gas adsorption (pores 0.4–1.5 nm) with density functional theory (DFT) evaluation and N$_2$ gas adsorption with Brunauer–Emmet–Teller (BET) evaluation (pores >1.5 nm), as described by Kwon & Pignatello [52].

2.7. Leaching Tests

pH-adjusted batch–leaching tests were conducted for biochars produced from a selection of the most heavy-metal-rich feedstocks (DSS-1, DSS-2 and WT) and the reference feedstock (CWC) (Table 1). The leaching tests were done according to standard CEN EN 12,457 with the following modifications: MilliQ and HCl (1 M) was mixed with biochar samples in sealed flasks (50 mL) at a liquid-to-solid ratio (L/S) of 5, then shaken on a vertical shaking table (120 rpm) over a period of 72 hrs, after which the eluates were filtered using a cellulose filter paper (Whatman Blue Ribbon, 0.45 μm). Parallel tests were set up in which solution pH was changed by addition of HCl (1 M) to the following target pHs: unaltered, 7.0, 5.5, and 4.0. Target pHs were selected based on soil-acidity thresholds [53]. Titration curves were constructed for a series of time intervals (4, 8, 24, 48, 72, 92 and 144 hrs, Figure S2) to determine both the amount of acid needed for each individual sample to reach the target pH and times needed to account for slow buffering reactions (see Supplementary Materials Section SA for more details). The predetermined amount of HCl was added stepwise over the time span of the experiment to avoid a drop below target pH. Target pH was achieved within an error of ±30% for all the tests conducted.

2.8. Data Analysis

All concentrations reported are in dry weight (w/w). A selection of metal(oid)s (As, Cd, Cu, Cr, Ni, Pb, and Zn) was included for the main presentation and discussion of results. These were selected because their environmental presence is generally regulated due to their toxicity. These will henceforth be referred to as heavy metals (HMs). Data for other elements analysed are included in the Supplementary Materials and used as supporting parameters in the discussion when relevant.

Fixation rates (FR) were determined as the ratio between the concentration in the biochar (C_{BC}) and the concentration in the feedstock (C_F), adjusted by the yield of the biochar (Y_{BC}) in accordance with Chanaka Udayanga [38], as follows:

$$FR(\%) = \frac{C_{BC}\left(\mu g\,kg^{-1}\right) \times Y_{BC}(\%)}{C_F\left(\mu g\,kg^{-1}\right)} \times 100 \tag{2}$$

The leachable concentration ($C_{leachable}$) of a metal in the biochar was defined as the amount released during the leaching test per mass of biochar [21], as follows:

$$C_{leachable}\left(\mu g\,kg^{-1}\right) = \frac{C_w\left(\mu g L^{-1}\right) \times V_w(L)}{m_{BC}(kg)} \tag{3}$$

where C_W is the metal concentration in the leachate, V_W is the volume of the leachate, and m_{BC} is the mass of the biochar.

The total leachable fraction of a metal in the biochar ($F_{leachable}$) is expressed as $C_{leachable}$ relative to the total concentration in the biochar (C_{BC}) [21], as follows:

$$F_{leachable}(\%) = \left[\frac{C_{leachable}\left(\mu g\,kg^{-1}\right)}{C_{BC}\left(\mu g\,kg^{-1}\right)}\right] \times 100 \tag{4}$$

Emission factors in mg per tonne biochar produced were calculated using the carbon-balance approach [54,55]. Application of this method allows the quantification of the amount of flue gas produced ($V_{flue\,gas}$), which is combined with the measured concentration of a metal in the flue gas (C_{metal}), to produce emission factors (EF_{metal}) of the respective metal per mass of biochar produced Equation (5). For more details about this method, see Sørmo et al. [43].

$$EF_{metal}\left(mg\,tonne^{-1}\right) = C_{metal}\left(mg\,Nm^{-3}\right) \times V_{fluegas}\left(Nm^3\,tonne^{-1}\right) \tag{5}$$

For the *FR* and mass-balance calculations, the results used were from the digestion that gave the most complete extraction of the target element, i.e., the HNO_3-HF-digestion (Ba, Cd, Co, Cr, K, Mg, Mo, Na, Ni, P, Pb, S, Si, Sr, and V). However, for elements that potentially form precipitates with HF (As, Ca, Cu, Fe, Mg, and Zn), results from the HNO_3 digestion were used.

3. Results and Discussion

3.1. Heavy Metals in Waste Feedstocks

Concentrations of selected heavy metals in the different waste feedstocks are shown in Figure 1 and Table S1. The clean wood-chips feedstock had concentrations of As, Cd, Co, Cr, Cu, Ni, Pb, and Zn (0.0033 ± 0.0003, 0.058 ± 0.002, 0.054 ± 0.02, 0.08 ± 0.03, 0.88 ± 0.01, 0.18 ± 0.02, 0.13 ± 0.02 and 23 ± 2 mg kg^{-1} respectively) that were all below previously reported concentrations for similar wood residues from logging [56], and can thus be considered representative of background levels for virgin wood. The concentrations of the same elements were higher in all the waste feedstocks; the values ranged from 3 times to 5400 times greater, with the largest differences being in the amounts of As (300–5400 times) and Cr (300–1100 times).
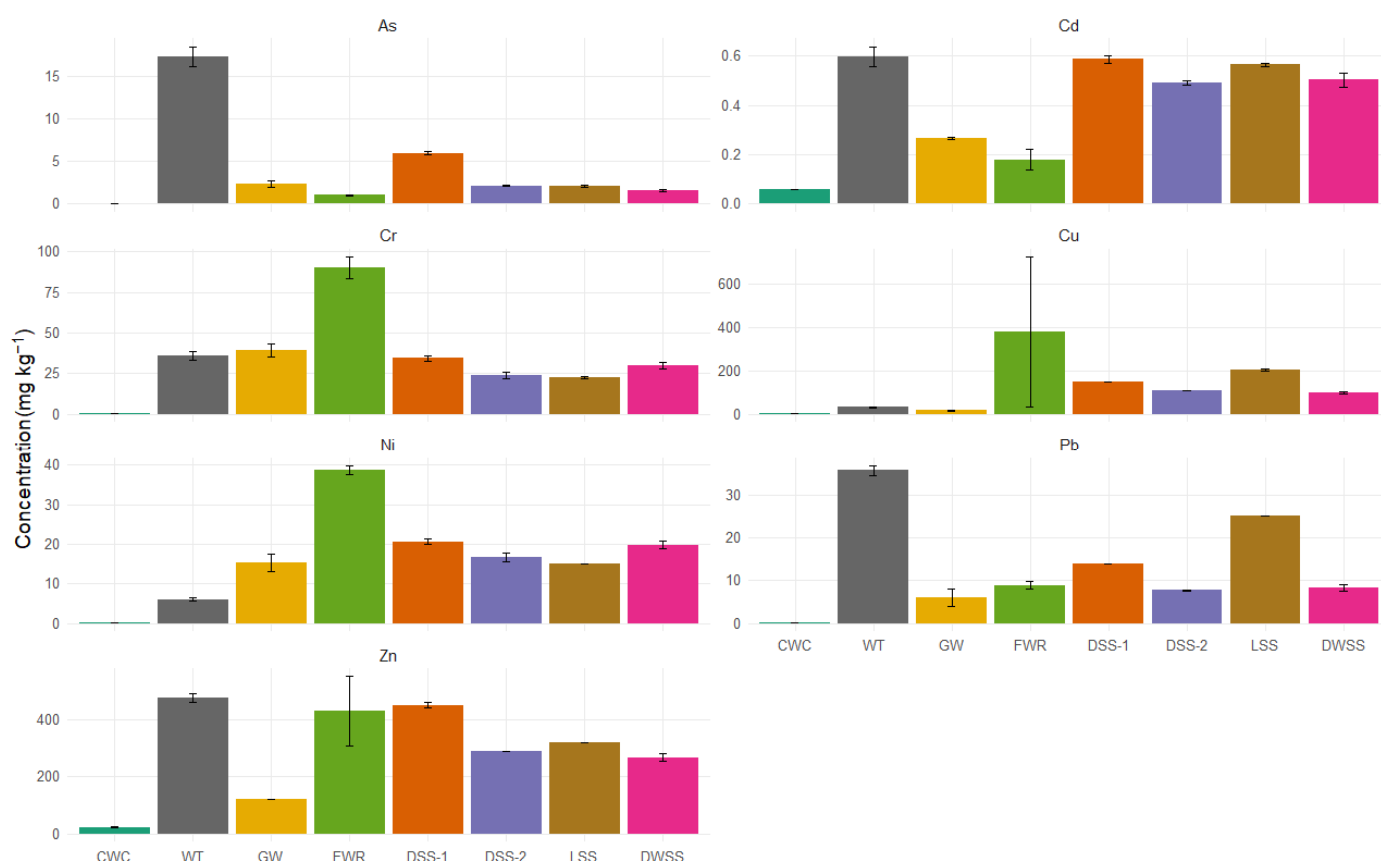
Figure 1. Concentrations of As, Cd, Cr, Cu, Ni, Pb, and Zn (mg kg^{-1}) in waste feedstocks before pyrolysis treatment (*n* = 3). CWC = clean wood chips, WT = waste timber, GW = garden waste, FWR = food-waste reject, DSS-1 and DSS-2 = digested sewage sludge, LSS = limed sewage sludge, and DWSS = de-watered sewage sludge.

The relatively high concentrations of As, Cd, Cr, Pb, and Zn (18 ± 1, 0.61 ± 0.04, 37 ± 3, 37 ± 1 and 491 ± 15 mg kg^{-1} respectively) in waste timber (WT) were similar to previously reported concentrations [21] and can be explained by the presence of metal objects, such as nails and staples, and inadvertently included chemically impregnated wood. The presence of impregnated wood would typically increase the concentrations of As, Cr, and Cu [23].

Elevated HM concentrations in food-waste reject, such as Cr (91 ± 7 mg kg^{-1}), Ni (39 ± 1 mg kg^{-1}), and Zn (434 ± 122 mg kg^{-1}), are likely the result of metal objects being discarded with the food waste in household recycling. Such objects are removed along with plastics during pre-treatment of food waste before anaerobic digestion and thus feature in the rejected-food-waste fraction. This was further observed by visual inspection and can explain the relatively large standard deviations of HMs in the FWR samples (Figure 1).

Garden soils, especially in urban areas, can be contaminated with heavy metals from diffuse sources, typically As, Cd, Pb, and Zn, resulting in uptake and elevated levels in plants grown in these soils [57,58] and thus in garden waste. Gravel and sand might also feature in garden waste, adding a geogenic contribution of HMs. Furthermore, the abrasive behaviour of this feedstock may result in increased wear on equipment used in contacting processes (dryer, pelletizer, etc.), resulting in contamination.

The concentrations in the sewage-sludge-based feedstocks (DSS-1, DSS-2, LSS, and DWSS, Figure 2) are all in the same range as those in sludge from diffuse domestic sources, as summarized by Agrafioti et al. [37]. The presence of heavy metals in sewage sludge is the result of an accumulation of particle-bound species during wastewater treatment, which typically scavenges 50–80% of the total HM content found in wastewater [59].
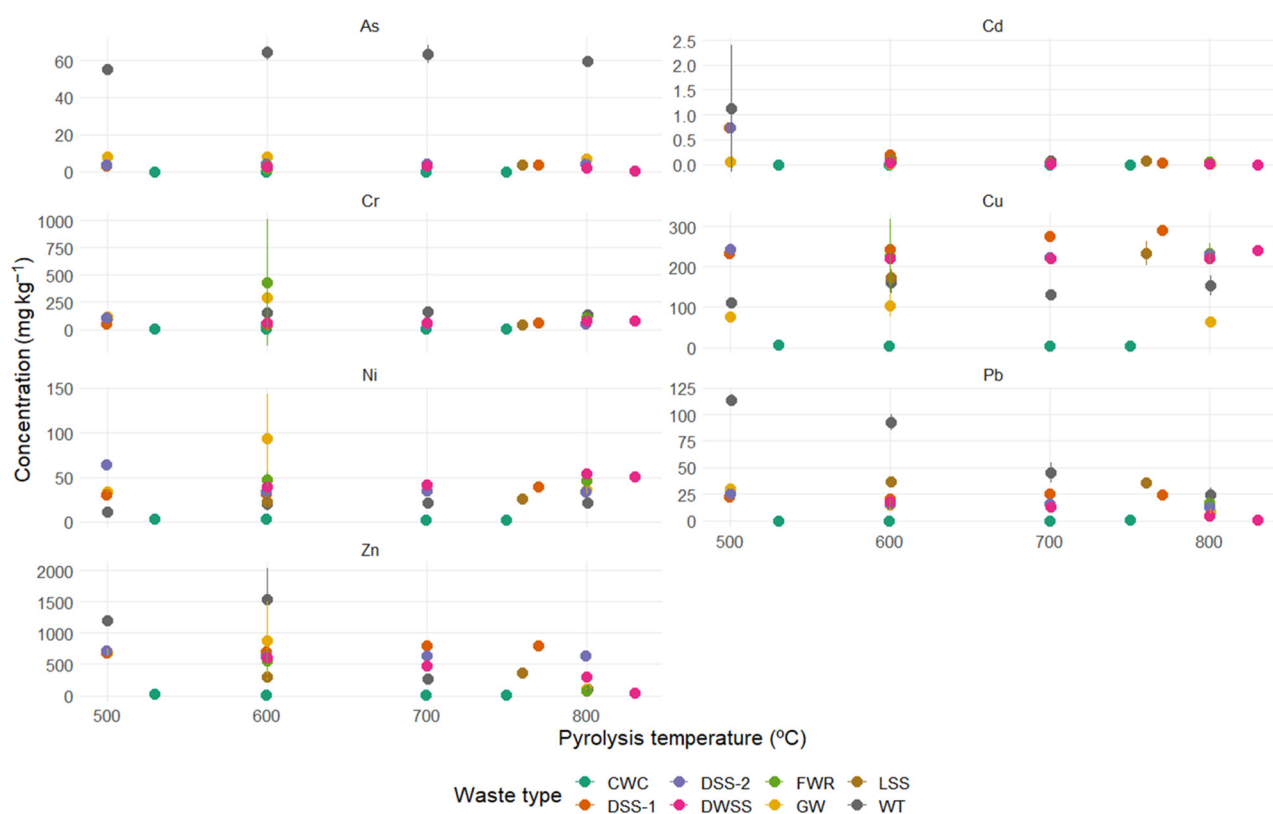
Figure 2. Concentrations of As, Cd, Cr, Cu, Ni, Pb, and Zn (mg kg^{-1}) in biochars produced from waste feedstocks at pyrolysis temperatures between 500 and 800 °C ($n = 3$). CWC = clean wood chips, WT = waste timber, GW = garden waste, FWR = food-waste reject, DSS-1 and DSS-2 = digested sewage sludge, LSS = limed sewage sludge, and DWSS = dewatered sewage sludge.

3.2. Biochar Characteristics

Pyrolysis (500–800 °C) produced a diverse set of biochar products from the 8 feedstocks (Tables S2 and S3). The wood-based feedstocks (CWC and WT) resulted in biochars with the lowest yields (16.9–32.1%), highest total carbon contents (79.6–92.5%), lowest ash contents (3.2–22.0%), and highest SSAs (449–715 m^2 g^{-1}, CO$_2$-sorption). The sewage sludge and food waste-based feedstocks (DSS-1, DSS-2, LSS, DWSS and FWR) on the other hand, gave the opposite set of characteristics, namely the highest yields (28.2–69.6%),

lowest carbon contents (10.5–32.3%), highest ash contents (69.1–93.4%) and the lowest SSA (70–205 $m^2 g^{-1}$, CO_2-sorption). Furthermore, these biochars contained the highest concentrations of P (7.4–47 g kg^{-1}), but other macronutrients, such as N, K, Mg, and Na were within the same ranges as in the wood-based and sludge-based biochars. Typically, woody materials contain few inorganic elements and are mainly composed of carbon-based structures such as cellulose, hemicellulose, and lignin, which are known to yield carbon-rich, porous biochars with low concentrations of metals [25,26]. Contrary to this, sewage sludges contain a wide variety of both volatile organic structures and inorganic elements that result in biochars with high ash and low carbon contents [26,35]. The digested and/or limed sewage sludge biochars (DSS-1, DSS-2 and LSS) furthermore contained high concentrations of Al (36–150 g kg^{-1}) and Fe (23–180 g kg^{-1}), a direct result of the use of flocculants such as $FeCl_3$ and $AlSO_4$ in the wastewater-treatment plants [60]. These two elements (Al and Fe) largely make up the differences observed in ash content between wood- and sludge-based biochars. The GW feedstock yielded biochars with properties in the ranges between those in the wood-based and sludge-based biochars, likely because this waste fraction is a mixture of woody residues and leaves with the addition of some sand and soil.

3.3. Heavy Metals in Waste Biochars

Biochar HM concentrations varied with both feedstock and pyrolysis temperature (Figure 2, Table S1). WT biochars had the highest concentrations of As, Cd, Pb, and Zn, and these were within the same order of magnitude as previously reported [21]. The relatively high concentrations of Cr and Ni in FWR (427 ± 583 and 47 ± 9 mg kg^{-1} respectively) and GW (290 ± 85 and 93 ± 50 mg kg^{-1} respectively), which were observed only in biochar made at 600 °C, were likely the result of feedstock heterogeneity (presence of metal fragments, see Section 3.1). For the biochars made from sewage-sludge-based feedstocks (DSS-1, DSS-2, LSS and DWSS), HM concentrations were similar to previously reported numbers [35,36], with the exception of Cd, the concentration of which was lower in the present study across all tested pyrolysis temperatures.

Based on average *FR*, disregarding temperature and matrix differences, the volatility of the HMs followed the subsequent order (Tukey's HSD test): Cd (*FR* = 10 ± 20%) > Zn (*FR* = 58 ± 39%) = Pb (*FR* = 67 ± 34%) = As (*FR* = 71 ± 25%) ≥ Cu (*FR* = 85 ± 23%) = Cr (*FR* = 92 ± 12%) = Ni (*FR* = 94 ± 10%). Detailed examination of the data for individual matrices and temperatures revealed that all biochars retained the majority of the original contents of Cr and Ni regardless of pyrolysis temperature (500–800 °C), as demonstrated by fixation rates (*FR*, Equation (2)) between 60 and 100% (see Table 2). A significant inverse relationship between HM concentration and pyrolysis temperature leading to *FR* between 0 and 35% was, however, observed for Cd in all biochars >500 °C, for Cu in FWR ≥600 °C, for Pb ≥700 °C in WT and ≥800 °C in DWSS, and for Zn at ≥700 °C in WT and ≥800 °C in GW, FWR, and DWSS. A number of studies on sewage-sludge pyrolysis reported the volatilization of both Cd and Pb (summarized by Udayanga et al., [22]), although at somewhat higher temperatures (>650 °C for Cd and >850 °C for Pb). Gong et al. [20] observed volatilization of Zn in contaminated plant residues above 500 °C, while Dong et al. [27] estimated volatilization of Zn to start at >700 °C by thermodynamic equilibrium calculations. These authors noted that the extent of volatilization would be matrix dependent. This is a likely explanation for why *FR* for Zn varied so much between feedstocks, for example the *FR* at 800 °C which was 4% for WT but 88% for DSS-2. Based on previous findings, As was expected to be one of the most volatile HMs, often with low *FR* even at temperatures < 500 °C [22,61]. Some degree of As volatilization was also observed in the present work, but *FR* were generally >60% for all treatment temperatures, with the exception of the DSS-1 feedstock (*FR* < 41% for all temperatures). The As retention in WT (*FR*: 63–100%), the feedstock with the highest As concentration (17 ± 1 mg kg^{-1}), mirrors numbers reported by Zhurinsh et al. [61] for CCA-impregnated wood (58–90%).

Table 2. Fixation rates (*FR*, %) for HMs in pyrolysis (500 and 800 °C) of CWC = clean wood chips, WT = waste timber, GW = garden waste, FWR = food-waste reject, DSS-1 and DSS-2 = digested sewage sludge, LSS = limed sewage sludge, and DWSS = dewatered sewage sludge.

Category	Feedstock	Pyr. Temp. (C)	As	Cd	Cr	Cu	Ni	Pb	Zn
Wood-based	CWC	530	100	0	100	100	100	22	21
		600	91	0	100	100	100	11	11
		700	70	0	100	100	100	13	3
		750	76	0	100	97	100	41	2
	WT	500	96	21	100	100	100	100	76
		600	100	3	100	100	94	86	87
		700	77	2	100	89	83	33	12
		800	63	1	80	92	70	13	4
	GW	500	100	6	97	100	95	100	100
		600	100	2	100	100	100	95	100
		800	70	3	64	97	79	100	22
Food-waste	FWR	600	59	9	96	21	100	100	46
		800	63	2	100	21	100	65	6
Sewage sludge & food-waste	DSS-1	500	33	65	95	97	97	87	95
		600	28	25	98	95	99	81	92
		700	33	4	100	100	100	100	100
		770	41	3	100	100	100	100	100
Sewage sludge	DSS-2	500	95	86	100	100	100	100	100
		600	83	8	99	86	100	90	92
		700	90	1	100	93	100	92	100
		800	82	1	83	84	100	67	88
	LSS	600	86	10	100	48	97	86	54
		750	98	1	62	62	97	79	61
	DWSS	600	66	2	77	88	78	82	89
		700	71	1	72	85	79	57	68
		800	40	1	83	73	89	18	35
		830	8	0	71	68	72	3	4

3.4. Heavy Metals in Pyrolysis Condensate

Heavy-metal contents (Cr, Cu, Ni, Pb, and Zn) were relatively low in all the pyrolysis-condensate samples (Table S5)—most of the samples had concentrations below or close to the LOD (1 mg kg^{-1}). Both Cu and Pb were detected in less than half of the samples, and the concentrations were all between 1 and 3 mg kg^{-1}. Zn concentrations were somewhat higher (1–49 mg kg^{-1}), with the highest levels found in the GW (6.3–44 mg kg^{-1}) and WT (1–49 mg kg^{-1}) samples. Heavy-metal content in pyrolysis condensates has not been widely reported, but the concentrations presented here are similar to those in the few earlier works [62–64]. Stals et al. [63] documented low concentrations of Cd (0.39–4.3 mg kg^{-1}), Pb (<0.5–1.1 mg kg^{-1}), and Zn (2.0–10.7 mg kg^{-1}) in pyrolysis condensates when pyrolyzing heavy-metal-contaminated biomass from phytoaccumulation tests at 350–450 °C. Similarly, Trinh et al. [64] found equally low concentrations of Cd (0.1–3.0 mg kg^{-1}) and Cr (0.2–0.5 mg kg^{-1}), and somewhat higher concentrations of Zn (2.3–97.8 mg kg^{-1}) in pyrolysis condensate from sewage sludges produced at 575 °C. In the present work, significant differences distinguished the condensates from sewage-sludge and wood-based feedstocks, however. Sewage-sludge pyrolysis produced condensates with more P (11–15 mg kg^{-1}) compared to wood-based feedstocks (<1–2 mg kg^{-1}), whereas pyrolysis of wood-based feedstocks yielded condensates with approximately 10–200 times more alkali and earth-alkaline metals (wood-based: Ca 84–159 mg kg^{-1}, K 8–10.4 mg kg^{-1}, Mg 60–87 mg kg^{-1}, and Na 157–197 mg kg^{-1}; sludge-based: Ca < 1–8 mg kg^{-1}, K < 1 mg kg^{-1}, Mg < 1 mg kg^{-1}, and Na < 1 mg kg^{-1}).

3.5. Heavy Metal Emission Factors

Emission factors (mg tonne^{-1}) of HMs from waste-feedstock pyrolysis (Equation (5)) are presented in Table 3. EF for further elements can be found in Table S6. Emission concentrations ($\mu g\,Nm^{-3}$) are summarized in Table S7. Heavy-metal emissions from the pyrolysis of the contaminated feedstocks (DSS-1, DSS-2, LSS, FWR, WT, and GW) were 1–2 orders of magnitude higher than those from pyrolysis of the reference material (CWC). Based on the mean sum of HMs for each feedstock, emission concentrations were as follows (high to low): FWR > GW > DSS-2 > WT > LSS > DSS-1. The highest emission concentrations were recorded for Cr (0.4–10.7 $\mu g\,m^{-3}$), followed by Ni (0.1–5.6 $\mu g\,m^{-3}$), Pb (0.02–5.6), and Zn (0.1–4.3 $\mu g\,m^{-3}$). No significant correlations ($p < 0.05$) between EF_{HM} and pyrolysis temperature were found for the individual feedstocks. An increase in EF with temperature was expected for volatile species, such as As, Cd, and Zn, but limitations of the sampling methodology might have confounded such results (see further discussion in Section 3.6). However, for 36 out of the 49 metal-feedstock combinations, the lowest EFs were observed at the lowest temperatures (500 and 600 °C).

Table 3. Flue gas emission factors (EF, mg tonne^{-1} of biochar produced) for heavy metals associated with aerosols (>0.45 μm) upon the pyrolysis (500–800 °C) of digested sewage sludge (DSS-1, DSS-2), limed sewage sludge (LSS), food-waste reject (FWR), waste timber (WT), garden waste (GW), and clean wood chips (CWC).

Category	Feedstock	Pyr. Temp. (°C)	Emission Factors EF (mg tonne^{-1})						
			As	Cd	Cr	Cu	Ni	Pb	Zn
Wood-based	CWC	530	0.21	n.d.	37	n.d.	0.01	0.01	28
		600	0.08	n.d.	17	2.6	22	n.d.	15
		700	0.10	n.d.	n.d.	0.04	0.40	0.02	29
		750	0.09	n.d.	1.5	11	0.09	0.51	41
	WT	500	1.8	0.03	11	9.6	3.9	6.1	8.3
		600	0.44	0.05	10	12	42	19	13
		700	0.79	0.21	111	16	102	34	28
		800	1.1	2.2	41	17	98	138	342
	GW	500	0.23	0.02	254	8.9	133	4.9	37
		800	3.3	0.13	111	3.6	35	129	85
Food waste	FWR	600	7.7	0.41	291	24	45	208	98
		800	8.9	0.19	251	15	143	184	110
Sewage sludge & food waste	DSS-1	500	0.16	0.0002	1.5	0.02	0.15	0.02	0.42
		600	0.92	0.001	13	0.13	1.5	0.44	1.0
		700	0.92	0.004	33	0.52	7.9	0.95	3.4
Sewage sludge	DSS-2	500	2.6	0.01	28	0.53	2.0	1.3	1.2
		600	3.9	0.12	78	4.0	5.6	17	7.5
		700	3.2	0.06	252	0.81	92	2.7	12
		800	3.9	0.05	48	2.2	9.5	3.7	14
	LSS	600	0.04	0.002	1.3	0.02	0.09	0.06	0.09
		760	8.1	0.55	208	2.4	46	43	69

Metal emissions from full-scale pyrolysis processes have not been widely quantified, so little or no literature is available for comparison. Our group has previously published emission concentrations and EFs for As, Cd, Cr, Cu, Pb, and Ni during the pyrolysis of one waste feedstock, WT, in a Pyreg-500 unit at one temperature, 600 °C [21]. In that study, emission concentrations from WT pyrolysis at 600 °C were in the same range as in the present work for As and Cd but 1–2 orders of magnitude higher for Cr, Cu, Ni, and Pb. Comparisons can, furthermore, be made to waste-incineration processes, for which emission regulations are in place. The observed measured sum of HMs emitted upon pyrolysis were 30–300 times lower than the EU threshold of 500 μg m^{-3} (Σ Sb + As+ Pb + Cr + Co +

Cu + Mn + Ni + V, see Table S7) for combustion plants with co-incineration of waste [65], although Mn and Sb data are lacking in the present work. Emission concentrations documented here (e.g., Cd: n.d.–0.03 µg m^{-3}, Pb: n.d.—5.6 µg m^{-3}, Zn: 0.1–4.3 µg m^{-3}) for all HMs investigated are also lower than previously reported values for fixed-bed biomass combustion (Cd: 0.2–10.1 µg m^{-3}, Pb: 3.4–124.8 µg m^{-3}, Zn: 646–7948 µg m^{-3}) [66].

3.6. Mass Balance for Heavy Metals in the Pyrolysis Process

When considering the mass balance of HMs in the pyrolysis of the waste fractions investigated (Cr, Cu, Ni, Pb, Zn; see Table S8), it is evident from the present work and previous studies [22,27,37,39] that the majority of HMs accumulate in the biochar. Median biochar-bound fractions, F_{BC}, across all feedstocks and pyrolysis temperatures were as follows: Cr: 88 ± 44%, Cu: 89 ± 21%, Ni: 94 ± 38%, Pb: 83 ± 51%, and Zn: 85 ± 44%. A negligible fraction ended up in the pyrolysis oil (median F_{PO} was 0.5 ± 0.2% for Cr, 0.0 ± 0.2% for Cu, 1.2 ± 1.2% for Ni, 0.0 ± 3.1% for Pb, and 0.1 ± 3.1% for Zn), as has previously also been noted by Gao et al. [67]. The fraction of HMs in the flue gas (F_{FG}, associated with aerosols >0.45 µm) represented an even smaller part of the total mass balance, with median F_{FG}- values of 0.1 ± 0.1% for Cr, 0.001 ± 0.009% for Cu, 0.03 ± 0.15% for Ni, 0.01 ± 0.28% for Pb, and 0.001 ± 0.023% for Zn.

However, when calculating the difference between the sum of HMs found in the three fractions (biochar, pyrolysis condensate and flue gas) and the original amount of HMs in the feedstock material (F_{diff}; HMs unaccounted for), this fraction ranged from −123.3 to 98.5%. It is hence obvious that the full mass balance is inaccurate and/or lacking. Inaccuracy likely stems from the feedstocks investigated being heterogeneous materials, with the large F_{diff} thus being the result of sampling error. At the same time, such sampling errors might disguise the fact that one or more of the fractions investigated were not properly quantified. Decreasing fixation rates with temperature (Table S4) indicate that an increasing fraction of Cd, Pb, and Zn should be found in either pyrolysis condensate or flue gas for several of the feedstocks with increasing treatment temperatures. Data for the pyrolysis condensates (Table S5) show that Pb and Zn do not accumulate in the condensate (no Cd-data is available for this fraction), but the amount measured in the flue-gas particles (>0.45 µm) did not reflect the increased volatilization of metals from the biochar matrix. A noteworthy example of this is Cd in WT pyrolyzed at 800 °C, for which F_{BC}, F_{PO}, and F_{FG} were 3.1, 0.1, and 0.001% respectively. It is speculated that this was due to HMs being present on ultra-fine particles (<0.45 µm), a phase that was not quantified in the present study. HMs have been found to increase with decreasing particle size in fly ash from lignite combustion [68]. Future work should therefore be directed towards quantifying HM emissions from pyrolysis associated with ultrafine particles.

3.7. Mobility of Heavy Metals in Biochars

Figure 3 presents the pH-dependent (unaltered pH, as well as pH 7, 5.5 and 4) leachable concentrations ($C_{leachable}$, Equation (3)) and leachable fractions ($F_{leachable}$, Equation (4)) of HMs from biochars produced from selected feedstocks (DSS-1, DSS-2, WT, and CW). Data are presented in full in the Supplementary Materials (Tables S9 and S10). The highest leachable concentrations were recorded at pH 4, and the lowest were recorded at the unaltered pH of the biochars (pH 8–12), as could be expected from the generally pH-dependent solubility of metals [69]. Considering $F_{leachable}$, it was evident that the HMs were most mobile in biochars made from wood-based feedstocks, CWC, and WT (Figure 3A). Despite having the lowest total HM concentrations, the CWC biochars generally had the highest $F_{leachable}$ (e.g., median $F_{leachable}$ of 26, 22, 32, and 54% for As, Cd, Ni, and Pb, respectively, across all pH). This is explained by wood-based biochars having lower ash contents, which means fewer mineral phases for the HMs to associate with (Table S3). This difference was particularly clear at pH 4, for which $F_{leachable}$ for As, Cd, Cr, Cu, Ni, Pb, and Zn were up to 100% for the wood-based biochars, but only up to 9.2% for the sewage-sludge-based biochars.

Figure 3. (**A**) Leachable concentrations (*n* = 3, mg kg⁻¹), and (**B**) leachable fraction (*n* = 3, %) of As, Cd, Cu, Cr, Ni, Pb, and Zn in biochars from clean wood chips (CWC), waste timber (WT), and digested sewage sludge (DSS-1 and DSS-2) made at pyrolysis temperatures 500–800 °C. pH = UA denotes the unaltered pH of the biochar.

Biochars made from WT had the highest $C_{leachable}$ for all HMs except Cu across the different feedstocks. However, $C_{leachable}$ increased by 2–3 orders of magnitude, with a reduction in pH from 9–12 to 4, as exemplified by Pb (0.019–0.045 mg kg^{-1} at pH 9–12, to 7–13 mg kg^{-1} at pH 4) and Zn (0.01–0.23 mg kg^{-1} at pH 9–12 to 24–433 mg kg^{-1} at pH 4). Despite total concentrations of HMs in CWC biochars being 1–3 orders of magnitude lower than those in the sewage sludge-based biochars, the $C_{leachable}$ of CWC, DSS-1 and DSS-2 biochars were all within the same order of magnitude, with the exception of the biochars produced at 500 °C.

Trends of $C_{leachable}$ with pyrolysis temperature varied with feedstock, pH, and the HM in question (Table S11). Cu, Pb, and Zn in WT, DSS-1 and DSS-2 were immobilized to an increasing degree (reduced $C_{leachable}$) with increasing pyrolysis temperature, which implies temperature-induced formation of low-solubility metal-matrix compounds, as has been suggested previously [38,40,41]. In the case of Zn, this effect could be linked to the formation of ZnO, ZnS, (Fe, Zn)S [38], and Al-silicates [27]. For Cu and Pb, the trends were mainly visible at low pH (4 and 5.5), as $C_{leachable}$ was marginal at higher pH levels. The increased insolubility of Cu could be due to the formation of low-solubility CuCl [38]. However, the HM-immobilization effect was in some cases limited at pH < 5.5, as WT correlated negatively with temperature in biochars leached at pH 7 and 5.5 (decreased leaching with temperature) but shifted to a positive correlation at pH 4 (increased leaching with temperature). In DSS-2, on the other hand, increased immobilization as a function of pyrolysis temperature was observed at all pH values. A reduction in As leaching with pyrolysis temperature has previously been linked to the formation of insoluble FeAs and CaAsO$_2$ [29,40]. The overall lower leaching of As observed for DSS-2 compared to WT could be due to formation of insoluble FeAs, as the DSS-2 feedstock is very Fe-rich (36 ± 2 g kg^{-1}) as compared to WT (1.1 ± 0.1 g kg^{-1}). Furthermore, Xu et al. [70] reported that the formation of reductive Fe-species, a prerequisite for FeAs formation, mainly happens upon the pyrolysis of feedstocks with significant amounts of labile carbon, such as sewage sludges.

The likelihood of HMs being immobilized in Fe-related mineral phases was also indicated by the correlation between Fe and HMs in the leachates (Figures S4 and S5). These correlations were strongest at pH 4, the point when the leachable concentrations were highest for both Fe and the HMs. Pearson correlation coefficients between Fe and As, Cd, Cu, Ni, and Pb at pH 4 were 0.57, 0.70, 0.76, 0.90, and 0.57, respectively (Figure S5).

3.8. Potential Applications

All the waste-feedstock biochars exceeded at least one European Biochar Certificate HM threshold value suggested for biochar for agricultural use (EBC-Agro) [31]; see Figure S3. For WT, As, Cd, Cr, Cu, and Zn-contents were too high, except for Cd in biochars produced above 500 °C and Zn in biochars produced above 700 °C. For all sewage-sludge biochars (DSS-1, DSS-2, LSS and DWSS), Cu and Zn concentrations exceeded threshold values, except for DWSS made at 800 °C. Biochars made from FWR and GW exceeded the EBC-Agro thresholds for Cr, Cu, Ni, and Zn in the biochars produced at 500 or 600 °C, in addition to Cu in FWR treated at 800 °C.

Judging by the heavy-metal premise of the EBC-Agro certification, only CWC and none of the contaminated feedstocks would be suitable for use to produce biochar for agricultural purposes. As discussed above (Section 3.7), however, HMs in the CWC biochars are more mobile compared to those in the sludge-based biochars. Despite large differences in the concentrations in the solid phase (Figure 2), the leachable concentrations of HMs from CWC biochars were in the same range as those from the sewage-sludge-based biochars (Figure 3A). This was due to the leachable fraction of HMs being much higher in CWC biochars (Figure 3B), a likely result of the HMs in these biochars not being immobilized in insoluble mineral phases to the same degree as those in the sewage-sludge-based biochars. To assess what metal mobility could signify for biochar soil application, a simplified calculation was performed, where the expected HM release from biochars added to an

acidic soil was assessed. The dose considered was 10 tonnes ha^{-1} based on work by van de Voorde et al. [71], for a worst-case scenario where post-application porewater pH is 4. For this scenario, HM leaching would be most extensive for WT biochars, due to both high HM concentrations and relatively high mobility (Figure 4). Most interestingly, however, the CWC, with the lowest solid-phase HM concentrations, would have a leaching of HMs that is either within the same order of magnitude or higher than that of DSS-1 and DSS-2 biochars if they are produced at pyrolysis temperatures $\geq 600\,°C$.
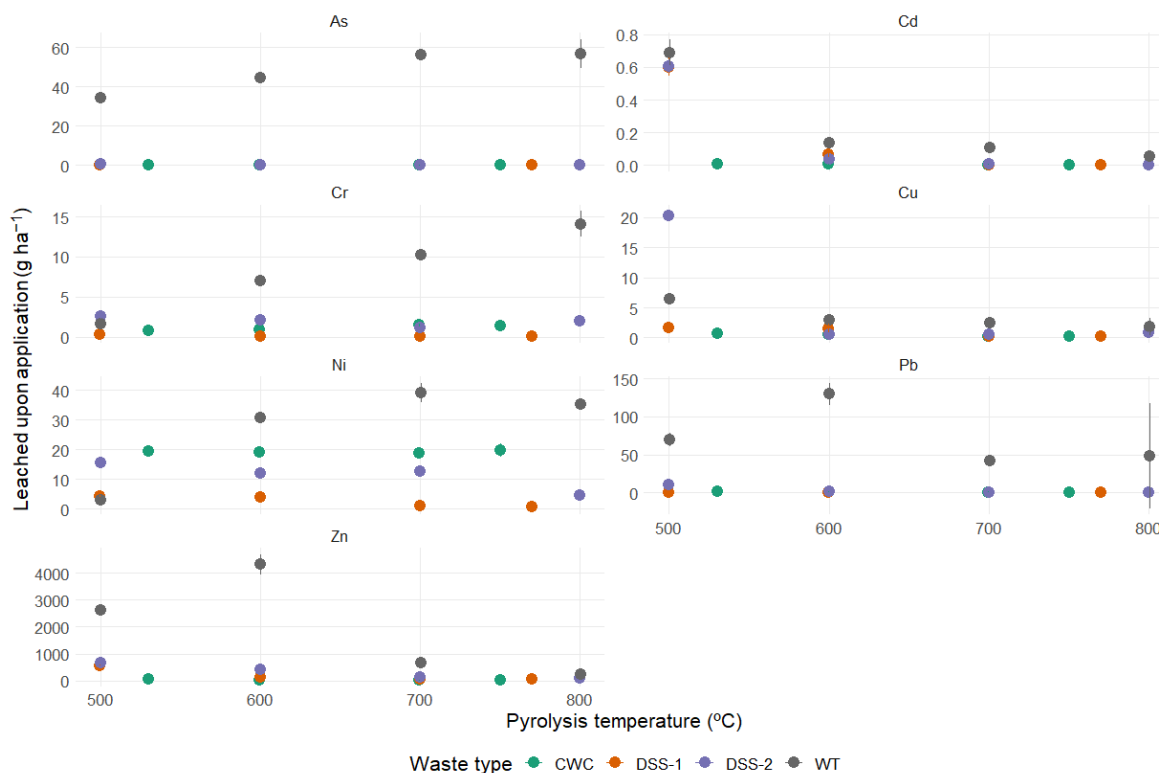
Figure 4. Theoretical amounts of As, Cd, Cu, Cr, Ni, Pb, and Zn leached (g ha^{-1}) from biochars made from clean wood chips (CWC), waste timber (WT) and digested sewage sludge (DSS-1 and DSS-2) made at different pyrolysis temperatures (°C) upon application to soil (10 t ha^{-1}) with a resulting soil porewater pH of 4.

This example clearly demonstrates the challenges posed by using total concentrations for threshold levels meant to assess environmental risk. In addition, the limited HM leaching from sewage sludge biochars implies that these could be suited for soil-improvement applications despite their relatively high total HM contents. It must be noted, however, that although pH is an important factor affecting HM mobility in soils, other parameters not considered here, such as complexation, sorption, and mechanical and microbiological weathering over time, can play a part. Future work should hence focus on long-term in situ studies.

4. Conclusions

Mass balances for HMs in products from the pyrolysis of organic wastes were established for an industrially relevant system. High fixation rates (>70%) were observed for most HMs studied, but As, Cd, Pb, and Zn partitioned into the flue gas at somewhat higher rates (*FR* < 30% for some feedstocks) at temperatures $\geq 600\,°C$. Low HM contents were observed in the pyrolysis condensates (<12%), with the highest concentrations documented for Zn (1–49 mg kg^{-1}). Computed emission factors (mg per tonne of biochar produced) for HMs in the flue gas were 0.04–7.7 for As, 0.002–0.41 for Cd, 0.01–208 for Pb, and 0.09–342 for Zn. The mobility of HMs in the biochars produced were much higher in the wood-based

biochars compared to the sludge-based biochars; at pH 4, up to 100% of HMs were leachable in the wood-based biochars, compared to up to 9.2% in the sewage sludge-based biochars.

To obtain biochars with both low HM content and low potential mobility from contaminated feedstocks, high pyrolysis temperatures (>600 °C) are required. High pyrolysis temperatures will subsequently potentially lead to HM emissions through the flue gas. Flue-gas cleaning is therefore recommended to reduce the potential environmental impact. Cyclones or bag filters can be used to scavenge HMs associated with particles, but as it is likely that a significant fraction of HMs is released with ultrafine particles (<0.45 μm), wet scrubbers, wet electrostatic precipitators or hybrid methods might be needed to achieve sufficient reduction in emissions [72].

Increased immobilization of HMs with increasing pyrolysis temperature is linked to the formation of insoluble mineral species, an effect that occurs to a larger extent in sewage-sludge-based biochars due to higher concentrations of inorganic compounds compared to wood-based feedstocks. This immobilization effect makes sewage-sludge biochars resistant towards HM leaching across a wide pH range, and to such a degree that their potential contribution of HMs to soils upon application might not necessarily be greater than that for biochars made from clean wood feedstocks. These results indicate the need to develop specific environmental-management thresholds for soil application of sewage-sludge biochars.

Leaching of HMs from sewage-sludge biochars and biochars made from other contaminated feedstocks should in future research be studied in situ to capture the effect of the complex chemical and mechanical weathering processes that can occur over time in different soil types. Also, future studies should attempt system analyses that weigh the benefits of biochar application against the potential release of HMs in an analysis similar to that done by Morales et al. [73]. This is probably necessary to determine the overall sustainability of value chains around biochar from HM-contaminated feedstocks for soil improvement or remediation.

Supplementary Materials: The following supporting information can be downloaded at: https://www.mdpi.com/article/10.3390/environments11060130/s1, Section SA: Leaching tests method development; Section SB: Supporting figures and tables; Figure S1: Schematic of the Biogreen pyrolysis system; Figure S2: Titration curves for CWC, WT, DSS-1, DSS-2 biochars produced at 600 C, repeated for different time intervals (4, 8, 24, 48, 72, 144, 192 hrs); Figure S3: Concentrations of As, Cd, Cr, Cu, Ni, Pb and Zn (mg kg^{-1}) in biochars produced from waste feedstocks at pyrolysis temperatures between 500 and 800 °C ($n = 3$). CWC = clean wood chips, WT = waste timber, GW = garden waste, FWR = food waste reject, DSS-1 and DSS-2 = digested sewage sludge, LSS = limed sewage sludge, and DWSS = de-watered sewage sludge. Dashed lines indicate threshold levels based on the EBC-agro quality criteria; Figure S4: Correlation matrix for elements (Ca, Fe, As, Cd, Cr, Cu, Pb, Ni, Zn) in eluates from leaching tests done at different pH levels (unaltered, 7, 5.5 and 4) for all biochars (CWC, WT, DSS-1, DSS-2); Figure S5: Correlation matrix for elements (Ca, Fe, As, Cd, Cr, Cu, Pb, Ni, Zn) in eluates from leaching tests done at pH 4 for all biochars (CWC, WT, DSS-1, DSS-2); Table S1:Concentrations of trace elements ($n = 3$, mg kg^{-1}) in feedstocks (0) and biochars produced at different pyrolysis temperatures (500–800 °C). Data for both HNO3, and HNO$_3$ + HF digestions; Table S2; Characterization data including pH, conductivity, ash, C, H, N and main elements for the feedstocks investigated and the resulting biochars; Table S3: Specific surface area (SSA) and pore volume (PV) for the biochars produced; Table S4: Fixation rates (*FR*, %) for main and trace elements in biochars from the pyrolysis of organic wastes at various temperatures; Table S5: Concentrations (ppm) of main and trace elements in condensate from the pyrolysis of digested sewage sludge (DSS-1, DSS-2), limed sewage sludge (LSS), food waste reject (FWR), waste timber (WT), and garden waste (GW) at temperatures between 500 and 800 °C. Samples analysed in triplicates shown as mean ± standard deviation; Table S6: Flue gas emission factors, EF (mg tonne-1) in the pyrolysis of DSS-1, DSS-2, LSS, WT, GW and CWC at various treatment temperatures (500–800 °C), in addition to $V_{flue\ gas}$ (m^3 kg^{-1}), as calculated through the carbon balance approach, used to derive EFs; Table S7: Flue gas emission concentrations (μg m^{-3}) in the pyrolysis of DSS-1, DSS-2, LSS, WT, GW and CWC at various treatment temperatures (500–800 °C); Table S8: Mass balance for main and trace elements showing the biochar (FBC), pyrolysis oil (FPO), flue gas (FFG) and the remaining difference

(F$_{diff}$) fractions in the pyrolysis of DSS-1, DSS-2, LSS, WT and GW at various treatment temperatures (500–800 °C); Table S9: Leachable concentrations (C$_{leachable}$, mg kg^{-1}) of selected heavy metals from biochars at different pH levels. UA = unaltered pH. Showing mean with standard deviation, and min and max range; Table S10: Leachable fractions (F$_{leachable}$, %) of selected heavy metals from biochars at different pH levels. UA = unaltered pH; Table S11: Linear regression analyses of how leachable concentrations of heavy metals (As, Ba, Cd, Co, Cr, Cu, Mo, Ni, Pb, Sr, V and Zn) correlate to pyrolysis temperature (500–800 °C) at different target pH levels (UA = unaltered pH of biochar, 7, 5.5 and 4). The references [42,43,74] were cited in the Supplementary Materials.

References

1. Beesley, L.; Moreno-Jiménez, E.; Fellet, G.; Melo, L.; Sizmur, T. Biochar and Heavy Metals. In *Biochar for Evnironmental Management: Science, Technology and Implementation*; Routledge: New York, NY, USA, 2015.
2. Lehmann, J.; Joseph, S. *Biochar for Environmental Management: Science, Technology and Implementation*, 2nd ed.; Routledge: New York, NY, USA, 2015.
3. Li, L.; Zou, D.; Xiao, Z.; Zeng, X.; Zhang, L.; Jiang, L.; Wang, A.; Ge, D.; Zhang, G.; Liu, F. Biochar as a Sorbent for Emerging Contaminants Enables Improvements in Waste Management and Sustainable Resource Use. *J. Clean. Prod.* **2019**, *210*, 1324–1342. [CrossRef]
4. Xiao, X.; Chen, B.; Chen, Z.; Zhu, L.; Schnoor, J.L. Insight into Multiple and Multilevel Structures of Biochars and Their Potential Environmental Applications: A Critical Review. *Environ. Sci. Technol.* **2018**, *52*, 5027–5047. [CrossRef] [PubMed]
5. Adhikari, S.; Timms, W.; Mahmud, M.A.P. Optimising Water Holding Capacity and Hydrophobicity of Biochar for Soil Amendment—A Review. *Sci. Total Environ.* **2022**, *851*, 158043. [CrossRef] [PubMed]
6. Obia, A.; Mulder, J.; Martinsen, V.; Cornelissen, G.; Børresen, T. In Situ Effects of Biochar on Aggregation, Water Retention and Porosity in Light-Textured Tropical Soils. *Soil Tillage Res.* **2016**, *155*, 35–44. [CrossRef]
7. Ippolito, J.A.; Spokas, K.A.; Novak, J.M.; Lentz, R.D.; Cantrell, K.B. Biochar Elemental Composition and Factors Influencing Nutrient Retention. In *Biochar for Environmental Management: Science, Technology and Implementation*; Routledge: New York, NY, USA, 2015.
8. Hale, S.E.; Nurida, N.L.; Jubaedah; Mulder, J.; Sørmo, E.; Silvani, L.; Abiven, S.; Joseph, S.; Taherymoosavi, S.; Cornelissen, G. The Effect of Biochar, Lime and Ash on Maize Yield in a Long-Term Field Trial in a Ultisol in the Humid Tropics. *Sci. Total Environ.* **2020**, *719*, 137455. [CrossRef] [PubMed]
9. Schmidt, H.-P.; Anca-Couce, A.; Hagemann, N.; Werner, C.; Gerten, D.; Lucht, W.; Kammann, C. Pyrogenic Carbon Capture and Storage. *GCB Bioenergy* **2019**, *11*, 573–591. [CrossRef]
10. Ahmad, M.; Rajapaksha, A.U.; Lim, J.E.; Zhang, M.; Bolan, N.; Mohan, D.; Vithanage, M.; Lee, S.S.; Ok, Y.S. Biochar as a Sorbent for Contaminant Management in Soil and Water: A Review. *Chemosphere* **2014**, *99*, 19–33. [CrossRef] [PubMed]
11. Alhashimi, H.A.; Aktas, C.B. Life Cycle Environmental and Economic Performance of Biochar Compared with Activated Carbon: A Meta-Analysis. *Resour. Conserv. Recycl.* **2017**, *118*, 13–26. [CrossRef]
12. Hale, S.E.; Arp, H.P.H.; Kupryianchyk, D.; Cornelissen, G. A Synthesis of Parameters Related to the Binding of Neutral Organic Compounds to Charcoal. *Chemosphere* **2016**, *144*, 65–74. [CrossRef]
13. Krahn, K.M.; Cornelissen, G.; Castro, G.; Arp, H.P.H.; Asimakopoulos, A.G.; Wolf, R.; Holmstad, R.; Zimmerman, A.R.; Sørmo, E. Sewage Sludge Biochars as Effective PFAS-Sorbents. *J. Hazard. Mater.* **2023**, *445*, 130449. [CrossRef]

14. Gupta, S.; Kua, H.W. Carbonaceous Micro-Filler for Cement: Effect of Particle Size and Dosage of Biochar on Fresh and Hardened Properties of Cement Mortar. *Sci. Total Environ.* **2019**, *662*, 952–962. [CrossRef] [PubMed]

15. Ritter, S.; Paniagua, P.; Hansen, C.B.; Cornelissen, G. Biochar Amendment for Improved and More Sustainable Peat Stabilisation. *Proc. Inst. Civ. Eng. Ground Improv.* **2022**, *177*, 129–140. [CrossRef]

16. Ye, L.; Peng, Z.; Wang, L.; Anzulevich, A.; Bychkov, I.; Kalganov, D.; Tang, H.; Rao, M.; Li, G.; Jiang, T. Use of Biochar for Sustainable Ferrous Metallurgy. *JOM* **2019**, *71*, 3931–3940. [CrossRef]

17. Anuar Sharuddin, S.D.; Abnisa, F.; Wan Daud, W.M.A.; Aroua, M.K. A Review on Pyrolysis of Plastic Wastes. *Energy Convers. Manag.* **2016**, *115*, 308–326. [CrossRef]

18. Barry, D.; Barbiero, C.; Briens, C.; Berruti, F. Pyrolysis as an Economical and Ecological Treatment Option for Municipal Sewage Sludge. *Biomass Bioenergy* **2019**, *122*, 472–480. [CrossRef]

19. Devi, P.; Saroha, A.K. Risk Analysis of Pyrolyzed Biochar Made from Paper Mill Effluent Treatment Plant Sludge for Bioavailability and Eco-Toxicity of Heavy Metals. *Bioresour. Technol.* **2014**, *162*, 308–315. [CrossRef]

20. Gong, X.; Huang, D.; Liu, Y.; Zeng, G.; Wang, R.; Wei, J.; Huang, C.; Xu, P.; Wan, J.; Zhang, C. Pyrolysis and Reutilization of Plant Residues after Phytoremediation of Heavy Metals Contaminated Sediments: For Heavy Metals Stabilization and Dye Adsorption. *Bioresour. Technol.* **2018**, *253*, 64–71. [CrossRef] [PubMed]

21. Sørmo, E.; Silvani, L.; Thune, G.; Gerber, H.; Schmidt, H.P.; Smebye, A.B.; Cornelissen, G. Waste Timber Pyrolysis in a Medium-Scale Unit: Emission Budgets and Biochar Quality. *Sci. Total Environ.* **2020**, *718*, 137335. [CrossRef]

22. Chanaka Udayanga, W.D.; Veksha, A.; Giannis, A.; Lisak, G.; Chang, V.W.-C.; Lim, T.-T. Fate and Distribution of Heavy Metals during Thermal Processing of Sewage Sludge. *Fuel* **2018**, *226*, 721–744. [CrossRef]

23. Helsen, L.; Van den Bulck, E. Metal Behavior during the Low-Temperature Pyrolysis of Chromated Copper Arsenate-Treated Wood Waste. *Environ. Sci. Technol.* **2000**, *34*, 2931–2938. [CrossRef]

24. He, M.; Xu, Z.; Sun, Y.; Chan, P.S.; Lui, I.; Tsang, D.C.W. Critical Impacts of Pyrolysis Conditions and Activation Methods on Application-Oriented Production of Wood Waste-Derived Biochar. *Bioresour. Technol.* **2021**, *341*, 125811. [CrossRef] [PubMed]

25. Kan, T.; Strezov, V.; Evans, T.J. Lignocellulosic Biomass Pyrolysis: A Review of Product Properties and Effects of Pyrolysis Parameters. *Renew. Sustain. Energy Rev.* **2016**, *57*, 1126–1140. [CrossRef]

26. Li, S.; Harris, S.; Anandhi, A.; Chen, G. Predicting Biochar Properties and Functions Based on Feedstock and Pyrolysis Temperature: A Review and Data Syntheses. *J. Clean. Prod.* **2019**, *215*, 890–902. [CrossRef]

27. Dong, J.; Chi, Y.; Tang, Y.; Ni, M.; Nzihou, A.; Weiss-Hortala, E.; Huang, Q. Partitioning of Heavy Metals in Municipal Solid Waste Pyrolysis, Gasification, and Incineration. *Energy Fuels* **2015**, *29*, 7516–7525. [CrossRef]

28. Han, H.; Hu, S.; Syed-Hassan, S.S.A.; Xiao, Y.; Wang, Y.; Xu, J.; Jiang, L.; Su, S.; Xiang, J. Effects of Reaction Conditions on the Emission Behaviors of Arsenic, Cadmium and Lead during Sewage Sludge Pyrolysis. *Bioresour. Technol.* **2017**, *236*, 138–145. [CrossRef] [PubMed]

29. Han, H.; Hu, S.; Lu, C.; Wang, Y.; Jiang, L.; Xiang, J.; Su, S. Inhibitory Effects of CaO/Fe2O3 on Arsenic Emission during Sewage Sludge Pyrolysis. *Bioresour. Technol.* **2016**, *218*, 134–139. [CrossRef] [PubMed]

30. Wang, J.; Tomita, A. A Chemistry on the Volatility of Some Trace Elements during Coal Combustion and Pyrolysis. *Energy Fuels* **2003**, *17*, 954–960. [CrossRef]

31. EBC. *European Biochar Certificate*; Version 8.2E.; European Biochar Foundation: Arbaz, Switzerland, 2012.

32. Huygens, D.; Saveyn, H.; Tonini, D.; Eder, P.; Delgado Sancho, L. *Technical Proposals for Selected New Fertilising Materials under the Fertilising Products Regulation (Regulation (EU) 2019/1009)*; EUR 29841 EN.; Publications Office of the European Union: Luxembourg, 2019. [CrossRef]

33. Sauvé, S.; Hendershot, W.; Allen, H.E. Solid-Solution Partitioning of Metals in Contaminated Soils: Dependence on pH, Total Metal Burden, and Organic Matter. *Environ. Sci. Technol.* **2000**, *34*, 1125–1131. [CrossRef]

34. Su, D.C.; Wong, J.W.C. Chemical Speciation and Phytoavailability of Zn, Cu, Ni and Cd in Soil Amended with Fly Ash-Stabilized Sewage Sludge. *Environ. Int.* **2004**, *29*, 895–900. [CrossRef]

35. Zhang, J.; Lü, F.; Zhang, H.; Shao, L.; Chen, D.; He, P. Multiscale Visualization of the Structural and Characteristic Changes of Sewage Sludge Biochar Oriented towards Potential Agronomic and Environmental Implication. *Sci. Rep.* **2015**, *5*, 9406. [CrossRef]

36. Lu, T.; Yuan, H.; Wang, Y.; Huang, H.; Chen, Y. Characteristic of Heavy Metals in Biochar Derived from Sewage Sludge. *J. Mater. Cycles Waste Manag.* **2016**, *18*, 725–733. [CrossRef]

37. Agrafioti, E.; Bouras, G.; Kalderis, D.; Diamadopoulos, E. Biochar Production by Sewage Sludge Pyrolysis. *J. Anal. Appl. Pyrolysis* **2013**, *101*, 72–78. [CrossRef]

38. Chanaka Udayanga, W.D.; Veksha, A.; Giannis, A.; Liang, Y.N.; Lisak, G.; Hu, X.; Lim, T.-T. Insights into the Speciation of Heavy Metals during Pyrolysis of Industrial Sludge. *Sci. Total Environ.* **2019**, *691*, 232–242. [CrossRef] [PubMed]

39. Kistler, R.C.; Widmer, F.; Brunner, P.H. Behavior of Chromium, Nickel, Copper, Zinc, Cadmium, Mercury, and Lead during the Pyrolysis of Sewage Sludge. *Environ. Sci. Technol.* **1987**, *21*, 704–708. [CrossRef] [PubMed]

40. Wang, J.; Takaya, A.; Tomita, A. Leaching of Ashes and Chars for Examining Transformations of Trace Elements during Coal Combustion and Pyrolysis. *Clean Coal Technol.* **2004**, *83*, 651–660. [CrossRef]

41. Jin, J.; Li, Y.; Zhang, J.; Wu, S.; Cao, Y.; Liang, P.; Zhang, J.; Wong, M.H.; Wang, M.; Shan, S.; et al. Influence of Pyrolysis Temperature on Properties and Environmental Safety of Heavy Metals in Biochars Derived from Municipal Sewage Sludge. *J. Hazard. Mater.* **2016**, *320*, 417–426. [CrossRef]

42. Berek, A.K.; Hue, N.V. Characterization of Biochars and Their Use as an Amendment to Acid Soils. *Soil Sci.* **2016**, *181*, 412–426. [CrossRef]

43. Sørmo, E.; Castro, G.; Hubert, M.; Licul-Kucera, V.; Quintanilla, M.; Asimakopoulos, A.G.; Cornelissen, G.; Arp, H.P.H. The Decomposition and Emission Factors of a Wide Range of PFAS in Diverse, Contaminated Organic Waste Fractions Undergoing Dry Pyrolysis. *J. Hazard. Mater.* **2023**, *454*, 131447. [CrossRef]

44. Sørmo, E.; Krahn, K.M.; Flatabø, G.Ø.; Hartnik, T.; Arp, H.P.H.; Cornelissen, G. Distribution of PAHs, PCBs, and PCDD/Fs in Products from Full-Scale Relevant Pyrolysis of Diverse Contaminated Organic Waste. *J. Hazard. Mater.* **2023**, *461*, 132546. [CrossRef]

45. SSB. Norwegian Waste Accounts for 2021. 2022. Available online: https://www.ssb.no/en/natur-og-miljo/avfall/statistikk/avfallsregnskapet (accessed on 17 April 2023).

46. Buss, W. Pyrolysis Solves the Issue of Organic Contaminants in Sewage Sludge While Retaining Carbon—Making the Case for Sewage Sludge Treatment via Pyrolysis. *ACS Sustain. Chem. Eng.* **2021**, *9*, 10048–10053. [CrossRef]

47. Castro, G.; Sørmo, E.; Yu, G.; Sait, S.T.L.; González, S.V.; Arp, H.P.H.; Asimakopoulos, A.G. Analysis, Occurrence and Removal Efficiencies of Organophosphate Flame Retardants (OPFRs) in Sludge Undergoing Anaerobic Digestion Followed by Diverse Thermal Treatments. *Sci. Total Environ.* **2023**, *870*, 161856. [CrossRef] [PubMed]

48. Moško, J.; Pohořelý, M.; Cajthaml, T.; Jeremiáš, M.; Robles-Aguilar, A.A.; Skoblia, S.; Beňo, Z.; Innemanová, P.; Linhartová, L.; Michalíková, K.; et al. Effect of Pyrolysis Temperature on Removal of Organic Pollutants Present in Anaerobically Stabilized Sewage Sludge. *Chemosphere* **2021**, *265*, 129082. [CrossRef] [PubMed]

49. Flatabø, G.Ø.; Cornelissen, G.; Carlsson, P.; Nilsen, P.J.; Tapasvi, D.; Bergland, W.H.; Sørmo, E. Industrially Relevant Pyrolysis of Diverse Contaminated Organic Wastes: Gas Compositions and Emissions to Air. *J. Clean. Prod.* **2023**, *423*, 138777. [CrossRef]

50. Nelson, D.W.; Sommers, L.E. Total Carbon, Organic Carbon and Organic Matter. In *Methods of Soil Analysis Part 2 Chemical and Microbiological Properties*; Page, A.L., Miller, R.H., Keeney, D.R., Eds.; American Society of Agronomy: Madison, WI, USA, 1982; pp. 539–579.

51. Bremmer, J.M.; Mulvaney, C.S. Nitrogen-Total. In *Methods of soil analysis Part 2 Chemical and Microbiological Properties*; Page, A.L., Miller, R.H., Keeney, D.R., Eds.; American Society of Agronomy: Madison, WI, USA, 1982; pp. 595–624.

52. Kwon, S.; Pignatello, J.J. Effect of Natural Organic Substances on the Surface and Adsorptive Properties of Environmental Black Carbon (Char): Pseudo Pore Blockage by Model Lipid Components and Its Implications for N2-Probed Surface Properties of Natural Sorbents. *Environ. Sci. Technol.* **2005**, *39*, 7932–7939. [CrossRef] [PubMed]

53. Johnston, A.E. Soil Acidity—Resilience and Thresholds. In *Managing Soil Quality—Challenges in Modern Agriculture*; CABI Publishing: Wallingford, UK, 2004; Chapter 3; pp. 35–45.

54. Bailis, R.; Ezzati, M.; Kammen, D.M. Greenhouse Gas Implications of Household Energy Technology in Kenya. *Environ. Sci. Technol.* **2003**, *37*, 2051–2059. [CrossRef] [PubMed]

55. Sparrevik, M.; Adam, C.; Martinsen, V.; Jubaedah; Cornelissen, G. Emissions of Gases and Particles from Charcoal/Biochar Production in Rural Areas Using Medium-Sized Traditional and Improved "Retort" Kilns. *Biomass Bioenergy* **2015**, *72*, 65–73. [CrossRef]

56. Bożym, M.; Gendek, A.; Siemiątkowski, G.; Aniszewska, M.; Malaťák, J. Assessment of the Composition of Forest Waste in Terms of Its Further Use. *Materials* **2021**, *14*, 973. [CrossRef] [PubMed]

57. Cheng, Z.; Lee, L.; Dayan, S.; Grinshtein, M.; Shaw, R. Speciation of Heavy Metals in Garden Soils: Evidences from Selective and Sequential Chemical Leaching. *J. Soils Sediments* **2011**, *11*, 628–638. [CrossRef]

58. Wong, J.W.C. Heavy Metal Contents in Vegetables and Market Garden Soils in Hong Kong. *Environ. Technol.* **1996**, *17*, 407–414. [CrossRef]

59. Kirk, P.W.W.; Lester, J.N. Significance and Behaviour of Heavy Metals in Wastewater Treatment Processes IV. Water Quality Standards and Criteria. *Sci. Total Environ.* **1984**, *40*, 1–44. [CrossRef]

60. Lee, C.S.; Robinson, J.; Chong, M.F. A Review on Application of Flocculants in Wastewater Treatment. *Process Saf. Environ. Prot.* **2014**, *92*, 489–508. [CrossRef]

61. Zhurinsh, A.; Zandersons, J.; Dobele, G. Slow Pyrolysis Studies for Utilization of Impregnated Waste Timber Materials. *J. Anal. Appl. Pyrolysis* **2005**, *74*, 439–444. [CrossRef]

62. Gao, N.; Quan, C.; Liu, B.; Li, Z.; Wu, C.; Li, A. Continuous Pyrolysis of Sewage Sludge in a Screw-Feeding Reactor: Products Characterization and Ecological Risk Assessment of Heavy Metals. *Energy Fuels* **2017**, *31*, 5063–5072. [CrossRef]

63. Stals, M.; Carleer, R.; Reggers, G.; Schreurs, S.; Yperman, J. Flash Pyrolysis of Heavy Metal Contaminated Hardwoods from Phytoremediation: Characterisation of Biomass, Pyrolysis Oil and Char/Ash Fraction. *J. Anal. Appl. Pyrolysis* **2010**, *89*, 22–29. [CrossRef]

64. Trinh, T.N.; Jensen, P.A.; Dam-Johansen, K.; Knudsen, N.O.; Sørensen, H.R. Influence of the Pyrolysis Temperature on Sewage Sludge Product Distribution, Bio-Oil, and Char Properties. *Energy Fuels* **2013**, *27*, 1419–1427. [CrossRef]

65. EU. *Directive 2000/76/EC of the European Parliament and of the Council of 4 December 2000 on the Incineration of Waste*; European Parliament: Strasbourg, France, 2000.

66. Wiinikka, H.; Grönberg, C.; Boman, C. Emissions of Heavy Metals during Fixed-Bed Combustion of Six Biomass Fuels. *Energy Fuels* **2013**, *27*, 1073–1080. [CrossRef]

67. Gao, N.; Kamran, K.; Quan, C.; Williams, P.T. Thermochemical Conversion of Sewage Sludge: A Critical Review. *Prog. Energy Combust. Sci.* **2020**, *79*, 100843. [CrossRef]

68. Zhang, L.; Chen, Z.; Guo, J.; Xu, Z. Distribution of Heavy Metals and Release Mechanism for Respirable Fine Particles Incineration Ashes from Lignite. *Resour. Conserv. Recycl.* **2021**, *166*, 105282. [CrossRef]

69. Stumm, W.; Morgan, J.J. *Aquatic Chemistry: Chemical Equilibria and Rates in Natural Waters*, 3rd ed.; John Wiley & Sons Inc.: Hoboken, NJ, USA, 1995.

70. Xu, Z.; Wan, Z.; Sun, Y.; Cao, X.; Hou, D.; Alessi, D.S.; Ok, Y.S.; Tsang, D.C.W. Unraveling Iron Speciation on Fe-Biochar with Distinct Arsenic Removal Mechanisms and Depth Distributions of As and Fe. *Chem. Eng. J.* **2021**, *425*, 131489. [CrossRef]

71. van de Voorde, T.F.J.; Bezemer, T.M.; Van Groenigen, J.W.; Jeffery, S.; Mommer, L. Soil Biochar Amendment in a Nature Restoration Area: Effects on Plant Productivity and Community Composition. *Ecol. Appl.* **2014**, *24*, 1167–1177. [CrossRef]

72. Singh, R.; Shukla, A. A Review on Methods of Flue Gas Cleaning from Combustion of Biomass. *Renew. Sustain. Energy Rev.* **2014**, *29*, 854–864. [CrossRef]

73. Morales, M.; Arp, H.P.H.; Castro, G.; Asimakopoulos, A.G.; Sørmo, E.; Peters, G.; Cherubini, F. Eco-Toxicological and Climate Change Effects of Sludge Thermal Treatments: Pathways towards Zero Pollution and Negative Emissions. *J. Hazard. Mater.* **2024**, *470*, 134242. [CrossRef] [PubMed]

74. Martinsen, V.; Alling, V.; Nurida, N.; Mulder, J.; Hale, S.; Ritz, C.; Rutherford, D.; Heikens, A.; Breedveld, G.; Cornelissen, G. PH effects of the addition of three biochars to acidic Indonesian mineral soils. *Soil Sci. Plant Nutr.* **2015**, *61*, 821–834. [CrossRef]